Heliyon 9 (2023) e18311

Contents lists available at ScienceDirect

Heliyon

journal homepage: www.cell.com/heliyon

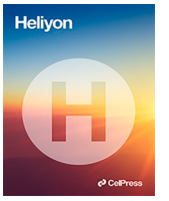

Theoretical insight on the optical centred electrical properties of guanidinium isophthalate NLO crystal for electro-optic Q switches

Paavai Era [a], RO. MU. Jauhar [a,*], T. Kamalesh [b], T. Prakash [a], V. Siva [c]

[a] Department of Physics, SIMATS School of Engineering, SIMATS, Chennai, 602 105, India
[b] Department of Physics, B.S. Abdur Rahman Crescent Institute of Science and Technology, Chennai, 600048, India
[c] Department of Physics, Karpagam Academy of Higher Education, Coimbatore, 641021, India

ARTICLE INFO

Keywords:
Organic NLO crystal
Growth parameters
Optical parameters
Optical luminescence
Laser tolerance

ABSTRACT

Guanidinium isophthalate single crystals with dimensions 16 × 4 x 2 mm^3 were prepared by the low temperature solvent evaporation method and growth kinetics with interfacial tension was discussed to bring out the growth parameters of guanidinium isophthalate single crystals. The harvested single crystals were utilized for various characterization studies like powder X-ray diffraction, optical transmission, photoluminescence, laser damage study and optical limiting studies. The visualization of varying potential regions on the surfaces to quantify short contacts were generated by Hirshfeld surface analysis. 2D fingerprint plots were analyzed, in which H ….H contact was found to be the most significant with 54.1%. Growth kinetics of the crystalline material was studied to reveal the nucleation process. Crystal samples prepared with reference to the solubility data were found to be free of inclusions and cracks and had maximum transmittance in the complete visible region. The electronic disorder of the crystal sample was reported in the form of Urbach energy. The PL spectra with the emission intensity provide the emission characteristic of the title compound. The major fundamental optical limit for a crystal material is experimentally measured and presented in the picosecond regime. Thus the present work contributes to the understanding of growth, structural, optical and electronic characteristics of the title guanidinium isophthalate single crystals for the fabrication of electro-optic devices in photonic industry.

1. Introduction

Organic nonlinear optical materials are focussed with much care because of their huge prompt nonlinear optical and electronic responses such as conductivity, susceptibility, high laser tolerance threshold and structural flexibility over inorganic crystalline materials. Nonlinear optical crystals are anticipated to design several potential optical information processors, telecommunication systems, frequency convertors, optical data storage and detection systems, etc [1]. In particular, the third generation nonlinear optical crystals possess a huge optical band gap and high laser damage threshold are in rich demand for their imaging, optical storage devices, spectroscopy, colour display units, optical communication systems etc., applications [2,3]. Experimental research outputs have been conceded over extensive period of study for the structural and optical properties of guanidine compound based crystals for their extensive influence in enhancing the utility of photonic devices in industrial applications. Though the aromatic and heteroaromatic

* Corresponding author.
E-mail address: jauharphysicist@gmail.com (RO.MU. Jauhar).

https://doi.org/10.1016/j.heliyon.2023.e18311
Received 1 June 2023; Received in revised form 12 July 2023; Accepted 13 July 2023
Available online 14 July 2023

polyfunctional carboxylic acid linkages in the structures of guanidinium salts are not found frequently in the literature survey, they still retain as area of interest owing to their capacity of generating stable supramolecular structural framework of guanidine cations by generating hydrogen-bonding associations through largely cyclic coordinates, viewed as those spotted in the structures of guanidinium carbonate and guanidinium bicarbonate [3,4]. To be specific, literature on guanidine complexes with benzenecarboxylic acid groups are being the central focus of attention because of their capacity of Linkage-Bridge between cation-anion networks. With this source of aspect, the present investigations were intended to synthesis and show the growth parameters and nucleation kinetics of the novel titular guanidinium isophthalate (GIP) single crystals. The grown GIP crystal structure and available compound details were identified and discussed using powder XRD analysis. The optical and electrical conductivity and linear susceptibility was generated from the experimental results of UV–Vis–NIR spectral analysis. To get further insight into the behaviour of GIP crystal in extreme high intensity laser regime, laser damage threshold and optical limiting studies have been performed and concluded that GIP crystal is several times better than the other well-known nonlinear optical (NLO) materials.

2. Experimental

2.1. Crystallization process

The crystalline product of GIP crystal was synthesized by raw precursors using slow evaporation method by adding guanidine carbonate to isophthalic acid in an equimolar ratio. The expected reaction scheme and the 3d structure of the crystalline compound is theoretically structured using chemdraw ultra and Gauss view 5.0 softwares respectively as shown in Fig. 1.

The precursors were purchased raw and made solution without any purification processes initially with aqueous methanol solvent. 200 mL of saturated solution was attained by continuous stirring of the precursors (guanidine carbonate and isophthalic acid) at room temperature. Homogeneous solution was attained in a course time of about 7 h continuous stirring. For purification, the as prepared solution is conventionally filtered using Whattman filtration method. Later, covered and perforated solution and left undisturbed to attain natural evaporation at room temperature. Specks of unevenly multinucleated crystals were noted over a span of 16 days. Repeated recrystallization was carried out until enhanced optical quality non-hygroscopic single crystals were harvested with high purity and transparency and the harvested GIP crystal with dimensions 16 × 4 × 2 mm^3 is shown in Fig. 2.

2.2. Solubility test

The process of crystallization is the impact of solubility dependant supersaturation rate of the compound. Finely powdered crystal salts of GIP were taken in bulk quantity and utilized for solubility studies at fixed temperature intervals of 5 °C ranging from 35 °C to 45 °C. The temperature of the prepared solution was constantly maintained using a ±0.01 °C accuracy rated CTB. Initially, the raw material was orderly performed for solubility study with 100 mL of the methanolic aqueous solution. Stirring was periodically carried out for 8 h at all temperatures to conserve homogeneous thermal distribution. Measured quantity of salt was added to 100 mL of the solvent continuously until supersaturation is achieved for each temperature respectively. Now, 10 mL of the measured saturated GIP solution from the retained temperature was pipetted and transferred into a petridish to dry out at ambience temperature. The dried solution produces multi nucleated crystalline powder. The crystalline powder is then weighed with correspondent concentrations. The procedure is repeated for various concentrations and the solubility concentration vs temperature plot is noted and marked in Fig. 3.

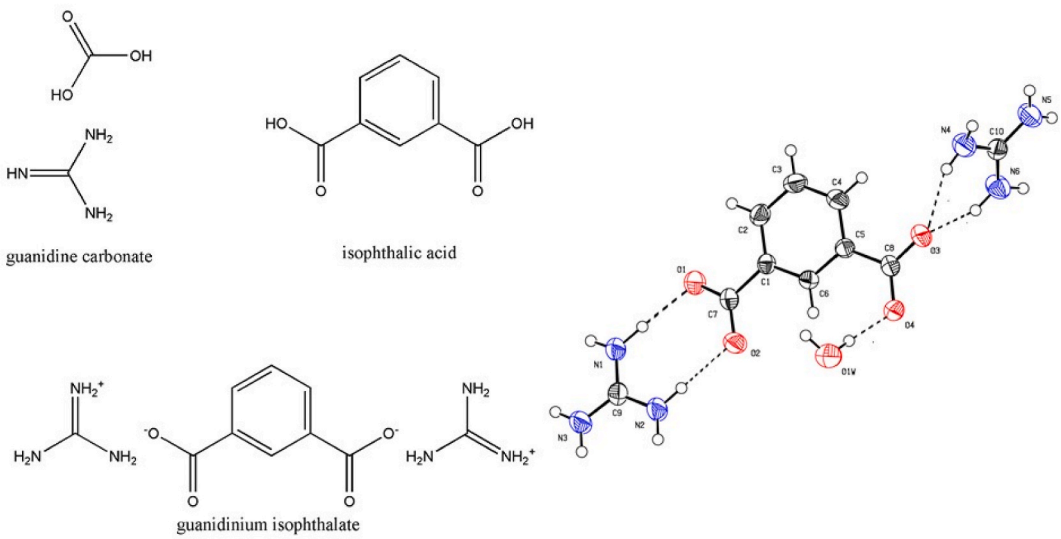

Fig. 1. Reaction scheme and 3d structure of GIP single crystal.

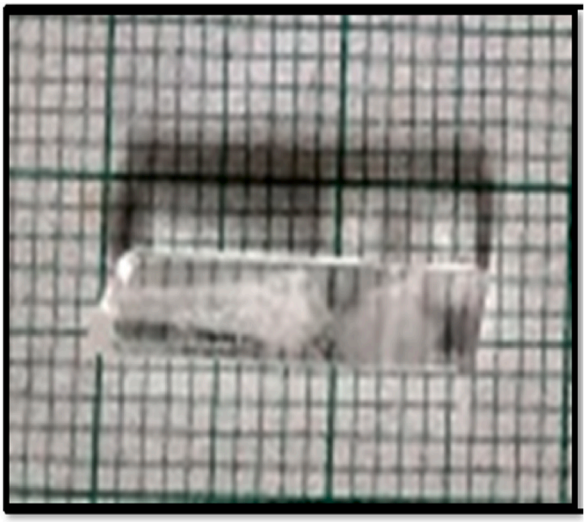

Fig. 2. As grown GIP crystal.

With reference to solubility plots and results, the saturated solution could be prepared to study growth kinetics of crystal nucleation.

2.3. Growth kinetics

Growth mechanism of GIP crystal compound is monitored and reported on the basis of nucleation speck and supersaturation rate. Conventional polythermal method is used to prepare the saturated solution and determine the zone width between saturation and supersaturation (otherwise known as metastable zone) [5]. The solubility data based definite temperature is maintained in the CTB with addition of 5 °C. The process of homogenous stirring was continued to spot the first visible crystal speck and the corresponding temperature was noted for this critical nucleus speck. The remaining concentrations from the solubility data was repeated with the same procedure. The reliable metastable zone width (MSZW) is shown in Fig. 4.

The minimum time taken to achieve a crystalline speck from a supersaturation solution at a definite temperature is called induction period and critically noted by isothermal method [6]. From Fig. 5, it is observed that the nucleation rate is increased exponentially with increasing temperature. This variation plot of supersaturation vs induction period determines the growth, optical quality and accurate morphology of the GIP crystalline sample by minimising the rate of spurious nucleation.

2.4. Interfacial tension of GIP

The theory of nucleation is identified with interfacial tension parameter of the prepared solution and growth kinetics. The current work is focused to calculate the homogeneous nucleation from interfacial tension on classical theory basis in order to determine the

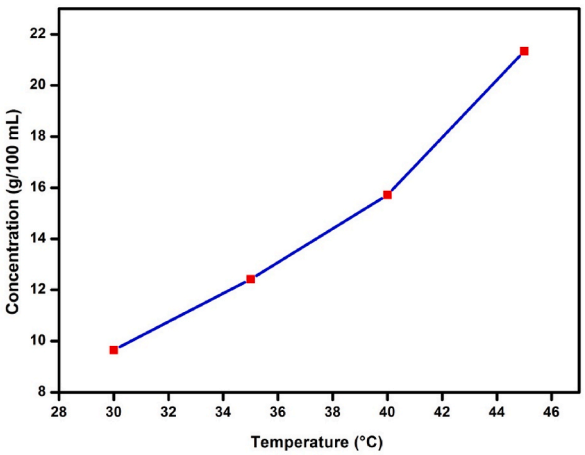

Fig. 3. Solubility curve of GIP in aqueous methanol solvent.

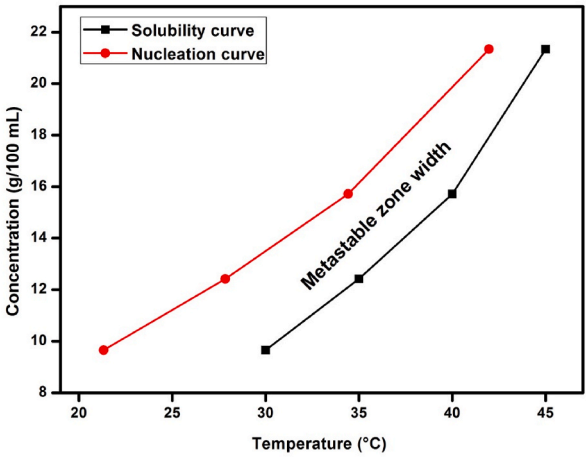

Fig. 4. Metastable zone width of GIP.

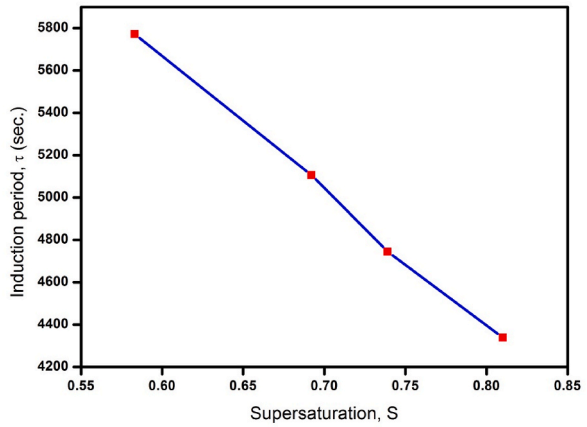

Fig. 5. Induction period Vs supersaturation of GIP crystal.

critical nucleation parameters [7]. The experimentally measured supersaturation concentration and induction period values are used in standard equations to bring out the interfacial tension at constant temperature. Fig. 6 shows the interfacial tension lying between crystal vs mother solution in terms of super saturation ratio. The interfacial tension values are calculated to be in the range of 2.24–4.73 mJ/m^2 in correspondence with the literature of nucleation studies [8]. In accordance with the classical homogenous

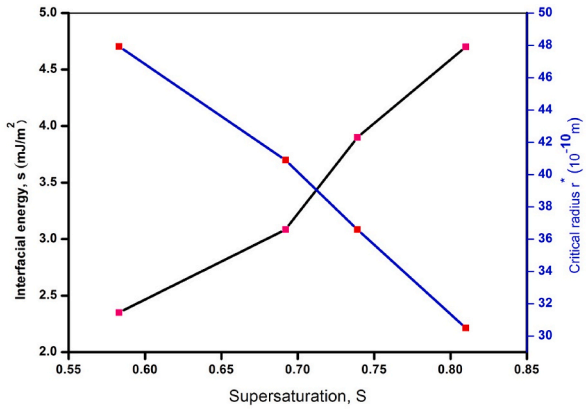

Fig. 6. Plot of supersaturation vs interfacial energy and critical radius for GIP crystal.

nucleation theory, the low value of growth rate implicated the larger probability of attaining good optical quality crystals from the mother solution. The required free energy and radius is calculated from the standard equations for the formation of critical spherical nucleus and the number of molecules bound in the critical nucleus. Table 1 provides the summarized values of nucleation kinetics parameter. The plot in Fig. 6 shows the calculated critical radius Vs supersaturation. From figure, the decreasing value of critical radius with the increasing supersaturation rate shows the availability of less number of molecules in the supersaturated mother solution.

3. Results and discussion

3.1. X-ray diffraction analysis

The crystal compound of the as-grown GIP single crystal was studied using Bruker D8 powder X-ray diffractometer with wavelength 1.5418 Å. A GIP crystal free of visual defects was crushed into powder and used for PXRD analysis. Fig. 7 exhibits the X-ray diffraction pattern of the powdered sample to confirm the crystalline phase of GIP crystal. From the spectral graph, it is perceived that the peak patterns are plotted from 10° to 30°. The results of the powdered crystal sample prove the single phase nature of the material supporting the literature [9]. From the clear broad well-defined peaks it is also proven that the crystals were free of inclusions. The structure of the title crystal was found to have $P2_1/n$ space group in the monoclinic crystal system and cell parameters a = 10.661, b = 11.501, c = 12.193, α = 90.000, β = 104.350, γ = 90.000, volume V = 1447.54 [9]. As shown in Fig. 8, the morphology of the as-grown crystal has well developed faces such as (1 0 0), (−1 0 0), (1 1 0), (-1-1 0), (0 0–1), (1-1-1), (−111) and (0 0 1).

3.2. Hirshfeld surface analysis

In the past decades, the molecular crystal structure analysis have been attempted beyond the present paradigm-internuclear distances, electronic structure densities, internuclear angles, crystal packing arrangements within molecular dynamics represented through hirshfeld surface models. Theoretical discussions on intermolecular interaction to view organic wholes and identification of deemed contacts with the experimental data are normally done by hirshfeld surface analysis [10]. The π–π intermolecular stacking interactions of crystal quantized by Crystal Explorer 3.1 provides the fingerprint plots (dnorm) and shape index. The Hirshfeld surface distance between the nearby nucleus by both inside and outside surface are their respective di and de bonds. Figs. 9 and 10 shows the Hirshfeld surface mapping finger plots over the GIP shape index. From Fig. 10, the H…H interactions occupies major contribution of 42.1% in the crystal structure whereas C–H, C–N, HO and N–H interactions being 0.3%, 9%, 0.3%, 8.6% and 0.3% respectively.

3.3. Electro-optic studies

Organic crystals of GIP prepared by conventional solvent evaporation method have a monoclinic structure. The optical anisotropic property of general symmetry structured molecular GIP crystals are characterized by UV–vis–NIR spectrum along (100) crystal plane. Recently we reported the molecular structure, nonlinear refractive index and thermal stability of organic molecular guanidinium isophthalate single crystals. The raw data shows a systematic molecular dispersion of the bound electronic nonlinearity near the two-photon absorption end. Knowledge of anisotropic refractive indices (n), extinction coefficient (k), optical conductivity (σ_{op}), electrical conductivity (σ_{el}), optical susceptibility (χ_{op}), electric susceptibility (χ_e) and optical polarizability (P) of the material are the required parameters for tailoring nonlinear optical waveguide devices. The analysis related the real and imaginary parts of the third order susceptibility are speculation demands of linear optical constants like absorption coefficient (α), refractive index and extinction coefficient. In literature, most studies primarily concentrate on the electronic bandgap which predicts real excitation. Our measurements on optical constants have been carried out with the knowledge of covalent bonded polarizabilities and electronic dependent bandgap obtained from the previous work [9]. We perform theoretical interpretations and outcomes to elaborate the optical constants from the relevant reflectance spectrum with corresponding transmittance vs wavelength is shown in Fig. 11. The below expressions are applied for the determination of refractive index and extinction coefficient [11].

$$R = \frac{1 \pm \sqrt{1 - \exp(-\alpha t) + \exp(\alpha t)}}{1 + \exp(-\alpha t)}$$

$$k = \frac{\lambda \alpha}{4\pi}$$

Table 1
Nucleation kinetic parameters of the GIP crystal.

Super saturation, S	Critical energy barrier, G* (10−20 J/m3)	Induction Period, τ (sec)	Interfacial Period, τ (mJ/m2)	MSZW, ΔT (K)
0.583	5,772.12	2.4	47.92	8.68
0.692	5,106.79	3.1	40.89	7.68
0.739	4,744.23	3.9	36.59	5.58
0.81	4,338.65	4.7	30.50	3.03

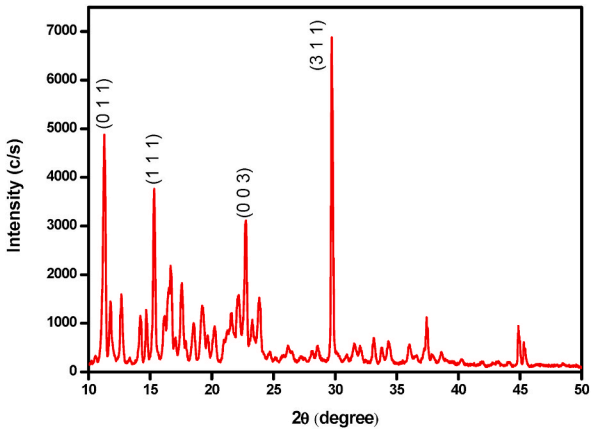

Fig. 7. Powder XRD pattern of GIP.

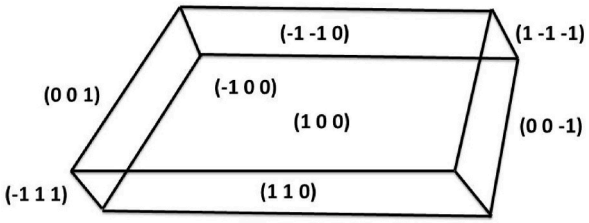

Fig. 8. Crystallographic planes of GIP.

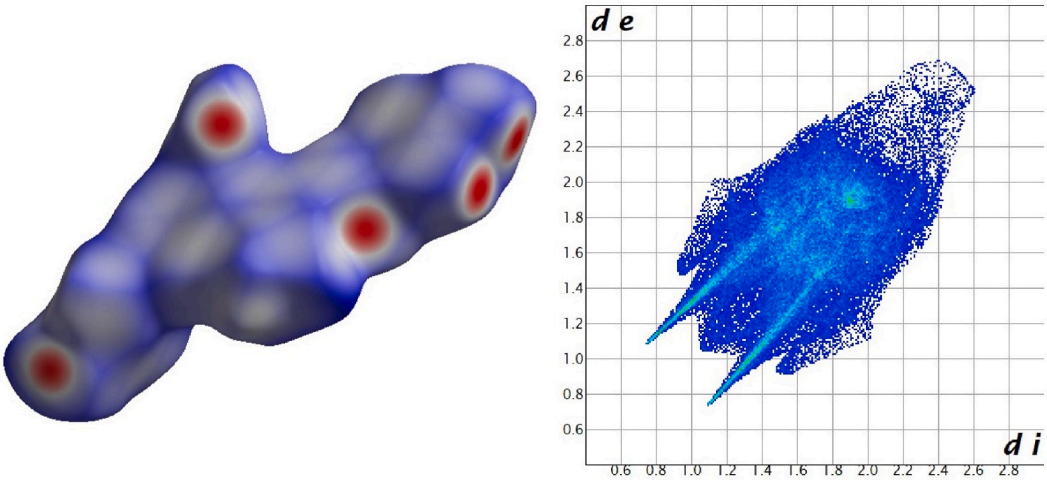

Fig. 9. Hirshfeld surfaces mapped over the surface of GIP.

$$n = \left\{ \frac{-(R+1) \pm \sqrt{-3R^2 + 10R - 3}}{2(R-1)} \right\}$$

where R is the experimentally measured reflectance. Obtained results for refractive index and extinction coefficient vs wavelength are depicted in Fig. 12. Fig. 11 illustrate that both the refractive index and extinction coefficient depend on the respective absorption coefficient as the internal efficiency of the optical device is required to suitably fit the α-value and Eg value for the intended fabrication of appropriate optoelectronic device fabrication [12]. The value of as measured refractive index of the GIP is found to be 1.3. It can be seen that the value of refractive index may be due to the reflectance edge which is responsible for direct bandgap of the material. Optical properties such as σ_{op}, σ_{el}, χe, χ_{op} and P are calculated from the following standard equations and the corresponding plots are

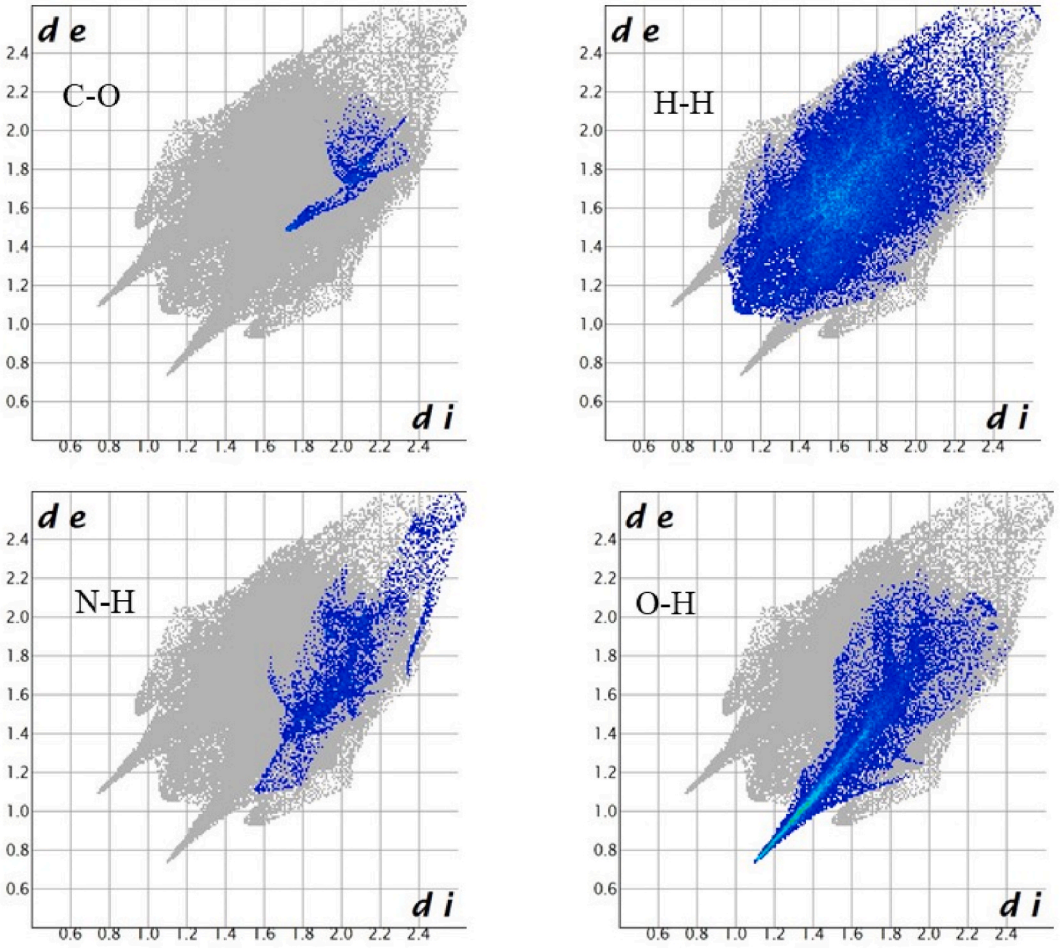

Fig. 10. C–O, H–H, N–H and O–H interactions in GIP crystal.

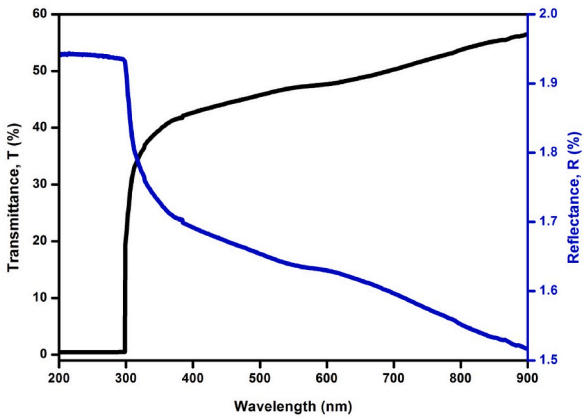

Fig. 11. Transmittance and reflectance spectrum of GIP crystal.

shown in Figs. 13–15 with respect to photon energy. The spectral graph shows that the optical conductance of the GIP compound increases with increasing photon energy which results in the dielectric behaviour of the sample crystal [13].

$$\sigma_{op} = \frac{\propto nc}{4\pi}$$

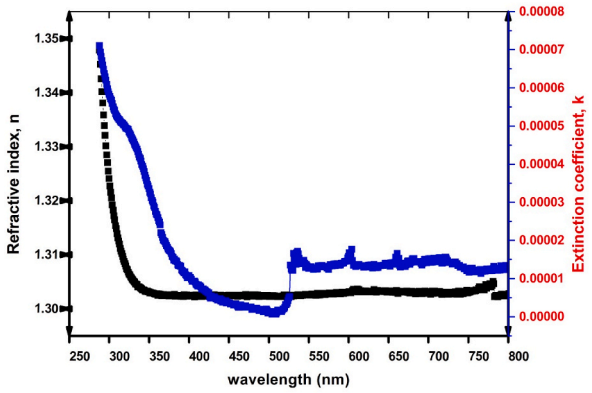

Fig. 12. Refractive index and extinction coefficient spectrum of GIP crystal.

$$\sigma_{el} = \frac{2\lambda\sigma_{op}}{\propto}$$

$$\chi = \frac{n^2 - k^2 - \varepsilon_0}{4\pi}$$

$$\chi = \frac{\varepsilon_0 hc\chi e}{\lambda}$$

$$P = \frac{\varepsilon_0 hc\chi_{op}}{\lambda}$$

where λ is the incident wavelength, ε_0 is the permeability in free space and χ_{op} is the optical susceptibility. From the theoretical formula, the electric susceptibility is calculated as 0.351 at 532 nm. The crystalline compounds with low defects inhibit the propagation of electromagnetic energy backed by its conductivity. The plot against photon energy between optical susceptibility and polarizability as seen from Fig. 15 claims that all the optical parameter values are maximum at the cut-off wavelength and vanish over optical band gap. The maximum optical values of the above mentioned parameters are observed from the energy gap. Hence from these observations we conclude that the dielectric nature of title crystal compound induces required polarization.

3.3.1. Urbach energy

Urbach energy (E_u) validates on the complexity of the tail level extensions in the forbidden E_g below the absorption edge. Urbach relationship exhibits the exponential dependence of absorption coefficient on the photon energy ($h\upsilon$) which is fundamentally related to the absorption edge of GIP compound [14].

$$\alpha(h\upsilon) = \alpha_0 \exp\left(\frac{h\upsilon}{E_u}\right)$$

where α_0 - constant, h - Planck's constant and υ - frequency. On increasing the crystallinity power, the slope at this section will also tends to increase and observed to be February 0, 6762 at the resultant stage. The slope value is obtained from the logarithmic linear plot of the absorption coefficient ($\ln(\alpha)$) versus $h\upsilon$ as shown in Fig. 16. The low quantitative value of slope interprets the high crystalline nature of the GIP sample. Reciprocate of the obtained slope in Fig. 16 depicts the E_u as 3.7366 eV for GIP compound by indicating the reduced structural defect in titular crystal [15].

3.4. Photoluminescence spectral study

The electronic and optical emission properties of crystalline compounds are experimentally resoluted from photoluminescence (PL) analysis. As illustrated in Fig. 17, the intensity of the emission spectrum with 311 nm excitation resulted in the emission spectrum with high intensity peak at 448 and 479 nm. The PL blue band at 448 and 479 nm with an excitation wavelength of 311 nm relates to the electronic transition from excited π^* state to ground state π. From the spectra of GIP crystal it is explicit that the title crystal is responsible for blue light emitting diodes [16].

3.5. Laser damage threshold study

Laser damage threshold study was carried out adopting laser-induced damage threshold to confirm the extent of radiation that a crystal can hold in the process of retaining its optical properties. Growth, optical, structural defect and geometric properties of the

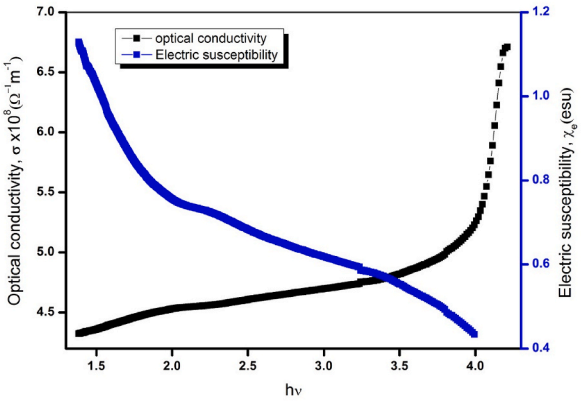

Fig. 13. Variation of optical conductivity and electric susceptibility vs hυ.

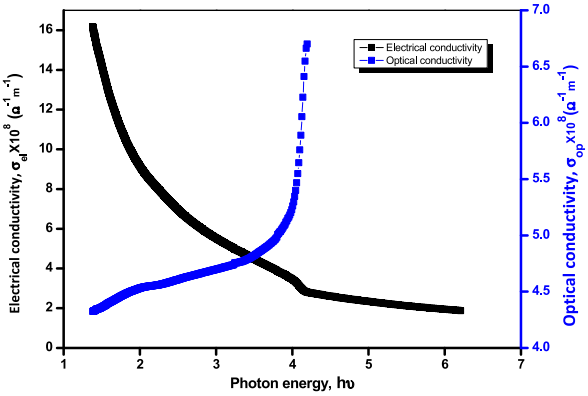

Fig. 14. Variation of electrical conductivity and optical conductivity versus hυ.

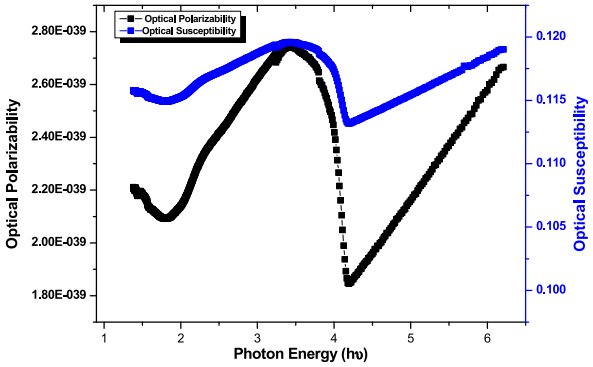

Fig. 15. Variation of optical polarizability and optical conductivity versus hυ.

crystalline material can also be exploited by incident laser beam. The crystal length and surface morphology of the crystal plays a vital role in determining the ability of the sample to with-hold the laser power. The optoelectronic and THz wave generation applications of nonlinear optical materials require information on the interaction of high intensity. This is to avoid the damage caused by laser beam thermal or other induced stress mechanism on the sensitive optical components resulting in dielectric breakdown. The characteristic property of the sample is measured from irradiated and irreversible peak power/fluence in the sample material. The experimental results of laser threshold is resoluted by illuminating high energy Q-switched Nd:YAG laser beam with wavelength 532 nm to the crystal sample placed at the biconvex focussed with focal length 15 cm. The standard pulse width repetition rate was fixed for 6 ns/10 Hz. The given input energy was maintained using a standard power meter. The variation in the power is gradually monitored until visible physical damage was detected on the crystal surface. The pertained digital values for the laser incident surface damage were

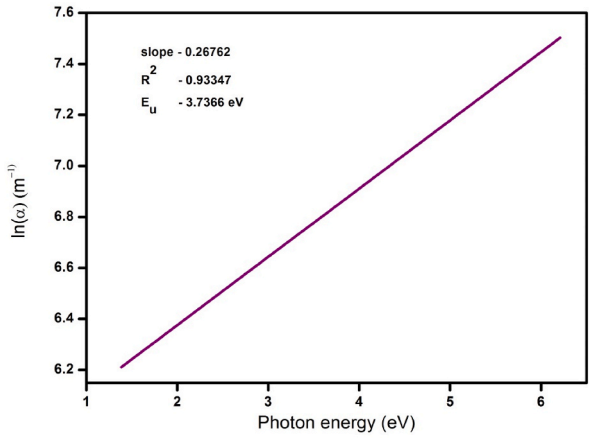

Fig. 16. Plot between hυ and ln(α) for the GIP crystal.

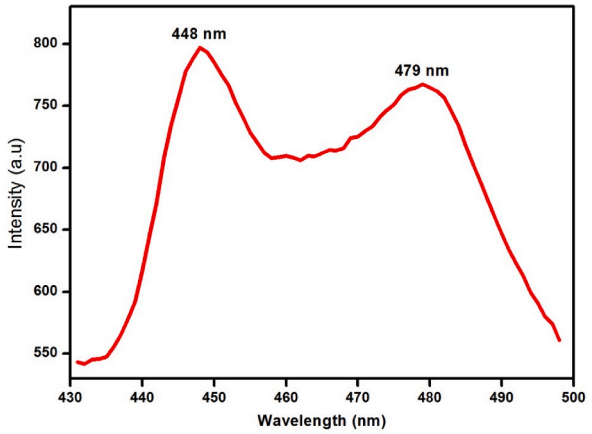

Fig. 17. Photoluminescence spectrum of GIP crystal.

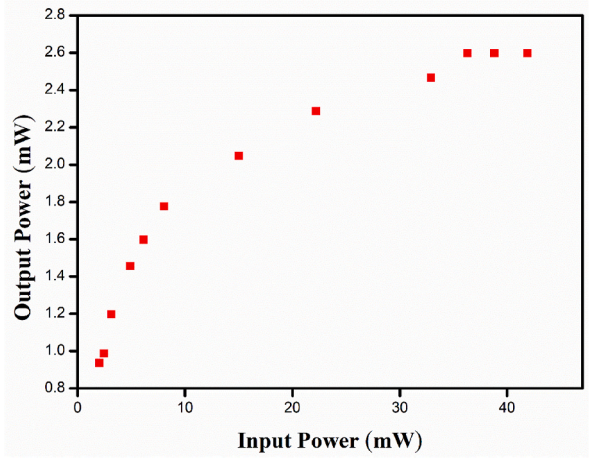

Fig. 18. Optical limiting behavior of GIP crystal.

utilized to determine the power density relation using the below relation;

$$\text{Power density } (P_d) = \frac{E}{\tau \pi r^2}$$

where E – threshold energy (mJ), τ-pulse width and r - radius of the laser beam spot. The power density at (100), (110) and (001) crystallographic planes were found to be 0.741, 2.043 and 2.196 GW/m^2 respectively. The obtained values of optical damage threshold show the maximum tolerance of the crystal at intended radiation and hence essentially inhibit the requirement of the GIP crystal for optical limiting device fabrications [17].

3.6. Optical limiting study

The optical limiting property of the crystalline compound is experimentally tested using a photo detector by providing measured input laser power of 10 mW to the respective samples via focusing lens. The experimental setup for optical limiting study is similar to that of Z scan setup with a power meter attached to it. The optical limiting behavior of the GIP crystal was measured using a photo detector by varying the laser power and recording the corresponding output power. The absorption at the probe wavelength and distance between sample to detector serves as the deciding factors of the output. These high intensified optical limiters are designed for the optimum utilization of the maximum transmittance with low level inputs [18,19]. The variation of output power vs input power is shown in Fig. 18. From the observations, the saturation threshold and amplitude was noted to be 36.327 mW/cm^2 and 2.585 mW/cm^2 respectively for their respective output and input power regions. An ideal limiter is demanded to provide safety to sensors or eyes below the regions of threshold [20]. Hence the as-grown GIP crystal can be nominated as a tailored candidate for optical limiting devices below their threshold.

4. Conclusion

Several new refinements and tailoring parameters have been discussed along with the literature to show the remarkable agreement required for the fabrication of a novel opto-electronic devices. The results of nucleation parameters provoke the attainment of well-defined crystal morphology with definite structural orientations. The crystalline confirmation was taken up by the experimentally observed sharp peaks from PXRD study. The hydrogen bonding interactions obtained from Hirshfeld analysis reveal the bonding nature in the grown crystal. Structural defects were also identified using Urbach relation calculated from the linear optical parameters of the GIP crystal. From the Luminescence property it is observed that emission of the GIP crystal is at 479 nm. The optical limiting study reveals that the threshold and amplitude was noted to be 36.327 mW/cm^2 and 2.585 mW/cm^2 respectively for their respective output and input power regions. The proposed electro-optic Q-switch application was justified with the promising out source of optical limiting and optical laser damage threshold organic molecule: guanidinium isophthalate single crystals.

Author contribution statement

Paavai Era: Conceived and designed the experiments; Wrote the paper.
RO. MU. Jauhar: Performed the experiments; Analyzed and interpreted the data.
T. Kamalesh; T. Prakash: Contributed reagents, materials, analysis tools or data.
V Siva: Performed the experiments.

Data availability statement

Data will be made available on request.

Declaration of competing interest

The authors declare that they have no known competing financial interests or personal relationships that could have appeared to influence the work reported in this paper.

References

[1] F.-A. Li, Q.-F. Tian, W.-C. Yang, S.-Z. Bai, A copper coordination polymer based on 3-(4-Hydroxypyridinium-1-yl) phthalic acid: synthesis and crystal structure, Synth. React. Inorg. Met. Nano-Metal Chem. 46 (2016) 268–273.
[2] T. Uma Devi, A. Josephine Prabha, R. Meenakshi, G. Kalpana, C. Surendra Dilip, Vibrational, electronic absorption, thermal and mechanical analyses of organic nonlinear optical material guanidinium phthalate, J. Mol. Struct. 1130 (2017) 472–479.
[3] J.M. Adams, R.W.H. Small, The crystal structure of guanidinium carbonate, Acta Crystallogr. B30 (1974) 2191–2193.
[4] D.A. Baldwin, L. Denner, T.J. Egan, A.J. Markwell, Structure of guanidinium bicarbonate: a model for the bicarbonate anion binding site of the transferrins, Acta Crystallogr. C42 (1986) 1197–1199.
[5] J. Nyvlt, R. Rychly, J. Gottfried, J. Wurzelova, Metastable zone-width of some aqueous solutions, J. Cryst. Growth 6 (1970) 151–162.
[6] N.P. Zaitseva, L.N. Rashkovich, S.V. Bagatyareva, Growth and Characterization of methyl-p-hydroxybenzoate (P-MHB) a non-linear optical material, J. Cryst. Growth 148 (1995).

[7] P.M. Ushasree, R. Muralidharan, R. Jayavel, P. Ramasamy, Metastable zonewidth, induction period and interfacial energy of zinc tris (thiourea) sulfate, J. Cryst. Growth 210 (2000) 741–745.
[8] K. Selvaraju, R. Valluvan, K. Kirubavathi, S. Kumararaman, Investigation on the nucleation kinetics of L-arginine acetate single crystals, Mater. Lett. 61 (2007) 3041–3044.
[9] Paavai Era, R.O.M.U. Jauhar, V. Viswanathan, G. Vinitha, P. Murugakoothan, Crystal structure, DFT and third order non-linear optical studies of an organic bisguanidinium isophthalate monohydrate single crystal, J. Mol. Struct. 1204 (2020), 127476.
[10] T. Hökelek, G.Ş. Aşkın, S. Özkaya, H. Necefoğlu, Crystal structure and Hirshfeld surface analysis of aquabis(nicotinamide-κ N 1)bis(2,4,6-trimethylbenzoato-κ O) zinc, Acta Crystallogr. Sect. E Crystallogr. Commun. 73 (2017) 1348–1352, https://doi.org/10.1107/S2056989017011690.
[11] R.W. Boyd, Nonlinear Optics, Academic Press, Newyork, 2003.
[12] R.O.M.U. Jauhar, G. Vinitha, P. Murugakoothan, Single crystal growth of bis guanidinium hydrogen phosphate monohydrate by Sankaranarayanan-Ramasamy method and investigation of its linear and nonlinear optical properties, J. Cryst. Growth 455 (2016) 90–93.
[13] P. Justin, K. Anitha, S.S.R. Inbanathan, G. Giester, M. Fleck, Growth, structural, thermal, mechanical, optical and third order nonlinear optical studies of 3-hydroxy 2-nitropyridine single crystal, Opt. Mater. 86 (2018) 562–570.
[14] F. Urbach, The long-wavelength edge of photographic sensitivity and of the electronic absorption of solids, Phys. Rev. 92 (1953) 1324.
[15] M. Subha, K. Anitha, R.O.M.U. Jauhar, The effect of malonic acid on the physico-chemical characterisation of 4-hydroxy pyridine: a new third order NLO single crystal, J. Mol. Struct. 1179 (2019) 469.
[16] W.L. Barros Melo, R.M. Faria, Appl. Phys. Lett. 67 (1995) 3892–3894.
[17] J.R. Krivacic, D.W. Urry, Ultraviolet refractive indices of aqueous solutions of urea and guanidine hydrochloride, Anal. Chem. 43 (11) (1971) 1508–1510.
[18] N.A. Romanyuk, B.V. Andriyevsky, N.N. Romanyuk, V.I. Stadnyk, The parameter of the optical indicatrix of guanidinium AluminumSulfate hexahydrate crystals, Opt Spectrosc. 116 (2) (2014) 249–253.
[19] G. Vinitha, A. Ramalingam, Laser Phys. 18 (2008) 1070–1073.
[20] Anandha Babu, P. Ramasamy, Spectrochim. Acta, Part A 82 (2011) 521–526.